

Newton's cradle analogue with Bose-Einstein condensates

Roberto Franzosi^{1,2} and Ruggero Vaia^{2,3}

¹ QSTAR and Istituto Nazionale di Ottica, Consiglio Nazionale delle Ricerche, largo Enrico Fermi 2, I-50125 Firenze, Italy

² Istituto Nazionale di Fisica Nucleare, Sezione di Firenze, via G. Sansone 1, I-50019 Sesto Fiorentino (FI), Italy

³ Istituto dei Sistemi Complessi, Consiglio Nazionale delle Ricerche, via Madonna del Piano 10, I-50019 Sesto Fiorentino (FI), Italy

E-mail: roberto.franzosi@ino.it

Abstract. We propose a possible experimental realization of a quantum analogue of Newton's cradle using a configuration which starts from a Bose-Einstein condensate. The system consists of atoms with two internal states trapped in a one dimensional tube with a longitudinal optical lattice and maintained in a strong Tonks-Girardeau regime at maximal filling. In each site the wave function is a superposition of the two atomic states and a disturbance of the wave function propagates along the chain in analogy with the propagation of momentum in the classical Newton's cradle. The quantum travelling signal is generally deteriorated by dispersion, which is large for a uniform chain and is known to be zero for a suitably engineered chain, but the latter is hardly realizable in practice. Starting from these opposite situations we show how the coherent behaviour can be enhanced with minimal experimental effort.

PACS numbers: 03.65.-w, 05.60.Gg, 03.75.Kk, 03.75.Mn

Submitted to: *J. Phys. B: At. Mol. Opt. Phys.*

1. Introduction

Classical machines represent a smart way to transmit insight of physical mechanisms concealed into nature. Quantum Mechanics has been one of the most prolific sources of unexpected phenomena, but is often hard to understand. Thus, finding a classical machine which is a paradigm for the quantum nature of a system is an engrossing challenge. Often, when one succeeds in fulfilling such a task, a plethora of phenomena intrinsic to the quantum nature can be observed and exploited to highlight the difference between the quantum and the classical realm.

In this work we trace a route towards the possible experimental realization of a quantum analogue of the Newton's cradle (NC) system: the analogy requires (i) a one-dimensional array of (ii) individual quantum systems, representing the spheres in the NC, and (iii) a nearest-neighbour interaction between them, modelling the contacts between the spheres. This last point is more evident if one thinks of a classical NC with spheres not in close contact but slightly separated: the momentum is transmitted between neighboring spheres in a short finite time and travels along the array towards the last sphere. Note that the beautiful experiment reported in [1] under the title *A quantum Newton's cradle* does not meet the above points, because what is observed there are the opposite-phase oscillations of two macroscopically populated coherent states created from a Bose-Einstein condensate within a single quasi-harmonic potential well. In other words the paper [1] is a fascinating demonstration of how coherent states are the quantum analogue of classical particles.

In order to meet the above requirements for realizing a quantum NC (QNC), we consider a collection of cold atoms trapped in a one-dimensional periodic potential, which can be built by confining a Bose-Einstein condensate in a one-dimensional tube that constrains it to a strict Tonks-Girardeau regime, whose first experimental realization has been reached in the remarkable experiment of [2], with a set-up closely similar to the one considered here. Superimposing a further optical potential of moderate amplitude along the longitudinal direction generates an optical lattice fulfilling condition (i). The dynamics of this system is effectively described by a one dimensional Bose-Hubbard model and, in the Tonks-Girardeau regime, the strong repulsive interaction between the atoms prevents the double occupancy of lattice sites. For the condensate we consider atoms with two possible internal states, say $|0\rangle$ and $|1\rangle$, like the hyperfine states of Rubidium atoms used in [3] to create entangled states; in this way each potential well hosts an effective two-state system (ii) and the wave-function at each lattice site is given by a superposition of these internal states. The tunnelling interaction between nearby wells, which can be globally tuned by the intensity of the optical lattice beam, provides the required coupling, which meets condition (iii).

In the following it is shown that a local perturbation generated at one end of the lattice propagates back and forth between the lattice ends in a very similar way to that in which an initial momentum pulse is periodically exchanged between the endpoint spheres of the classical NC: in fact, the role of the classical momentum Δp transferred

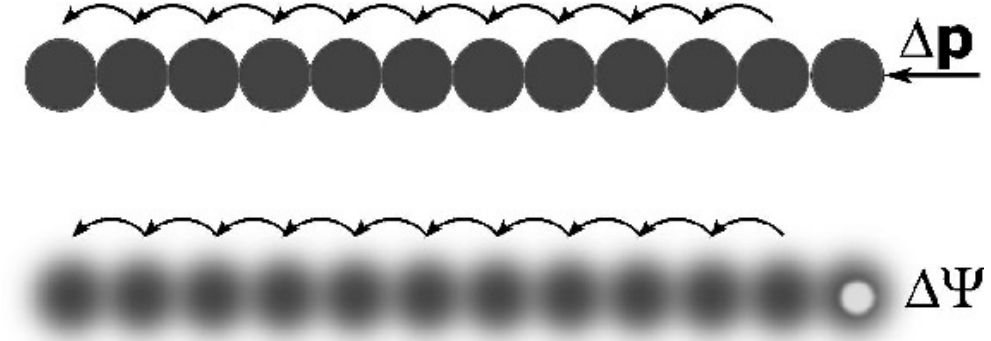


Figure 1. The analogy between the classical Newton's cradle, where the impulse of the mechanical momentum is transmitted along nearby spheres, and the realization through a Bose-Einstein condensate, where a wave-function disturbance is 'delivered' along the optical lattice.

between the chain ends is played now by the wave-function disturbance $\Delta\Psi$ which is transmitted through the system. In particular, we assume the lattice prepared with all sites in (say) the $|0\rangle$ state, and the initial disturbance $\Delta\Psi$ consists in changing the first site to the $|1\rangle$ state: the latter will propagate through the 'sea' of $|0\rangle$ states. The analogy is exemplified in figure 1.

The system and its dynamics are introduced in Section 2; in Section 3 we consider two antithetical cases: the simplest uniform lattice, with an unluckily poor dynamics, and the perfectly transmitting lattice, with individually constructed couplings. Note that in both these cases the net number-of-atoms transport is null, while a counterflow dynamics [4] is active. In fact, the currents of the two atomic internal states have the same intensity and opposite signs. Thus, in the case of the uniform lattice the counterflow is dissipative, and in the second setup a super-counter-fluidity is observed [4]. These two examples help to understand under which conditions signals are transported efficiently between the lattice ends and why in some cases they fade out. As realizing the second setup in the lab would be a strong challenge, we examine in Section 4 two arrangements that involve slight adjustments to the least demanding uniform lattice and yield very high dynamic quality. The results are summarized and discussed in Section 5.

2. The system

We consider a system of atoms with two internal states subjected to a strong transverse trapping potential with frequency $\omega_{\perp} \gg \mu/\hbar$, where μ is the chemical potential, with a further standing-wave laser beam applied so that a periodic potential in the longitudinal direction is created. For sufficiently strong transversal and longitudinal potential, and low temperatures, the atoms will be confined to the lowest Bloch band. The low-energy Hamiltonian is then given (see Appendix A) by the Bose-Hubbard model for two boson

species [4, 5, 6] labeled by $\alpha = 0, 1$:

$$\begin{aligned}
 H = & \sum_{\alpha=0}^1 \sum_{j=1}^M [U_{\alpha} \hat{n}_{\alpha j} (\hat{n}_{\alpha j} - 1) + \xi_j \hat{n}_{\alpha j}] \\
 & + U \sum_{j=1}^M (\hat{n}_{0j} - 1/2)(\hat{n}_{1j} - 1/2) \\
 & - \sum_{\alpha=0}^1 \sum_{j=1}^{M-1} t_{\alpha j} (\hat{a}_{\alpha j}^{\dagger} \hat{a}_{\alpha, j+1} + \text{h.c.}), \tag{1}
 \end{aligned}$$

where the index j runs on the lattice sites and the boson operator $\hat{a}_{\alpha j}$ ($\hat{a}_{\alpha j}^{\dagger}$) destroys (creates) an atom in the internal state α at the lattice site j . Boson commutation relations $[\hat{a}_{\alpha j}, \hat{a}_{\beta j'}^{\dagger}] = \delta_{jj'} \delta_{\alpha\beta}$ are satisfied and $\hat{n}_{\alpha j} = \hat{a}_{\alpha j}^{\dagger} \hat{a}_{\alpha j}$ is the boson number operator for the species α at site j . In the expression above, U and U_{α} are the inter- and intra-species on-site interaction energy, respectively, whereas $t_{\alpha j}$ is the amplitude for the species α to hop between sites j and $j+1$. It is realistic to assume that the site energy offsets ξ_j do not depend on the internal atomic state.

2.1. Effective dynamics in the Tonks-Girardeau regime

The homogeneous one-dimensional Bose-Hubbard model, has two remarkable dichotomous limits. In the case of a vanishing repulsion ($U = U_{\alpha} = 0$), the model described by Hamiltonian (1), reproduces two independent ideal Bose gases on a lattice. The case we are interested in is instead the opposite one, that is with a strong repulsive interaction ($U, U_{\alpha} \rightarrow \infty$) and with a number of atoms equal to the number of sites. In the latter case, an ideal Fermi gas is found. As a matter of fact, very high values of $U/t_{\alpha j}$ and $U_{\alpha}/t_{\alpha j}$, for $j = 1, \dots, M-1$, entail such a high amount of energy for accumulating more than one atom in a given site, that no site can be doubly occupied. Hence, assuming $U, U^{\alpha} \gg t_{\alpha j}$, the only observable states are those where the occupancy of any site is equal to one: $\hat{n}_{0j} + \hat{n}_{1j} = 1$. These states form a restricted Hilbert subspace \mathcal{H}_R . A first consequence of this constraint is that the offset term in (1), $\sum_j \xi_j$, is a constant that we may neglect.

The two possible one-atom states at site j can be written as $|0\rangle_j \equiv \hat{a}_{0j}^{\dagger} |00\rangle_j = |10\rangle_j$, and $|1\rangle_j \equiv \hat{a}_{1j}^{\dagger} |00\rangle_j = |01\rangle_j$, where $|00\rangle_j$ is the empty state for the j -th site: hence, $|0\rangle_j$ and $|1\rangle_j$ correspond to the j th atom in the internal state 0 or 1, respectively. In this way the dynamics is ruled by the only internal states and an effective Pauli exclusion is realized. More precisely, noting that double creation or annihilation are prohibited, i.e., $\hat{a}_{\alpha j}^{\dagger} \hat{a}_{\alpha' j}^{\dagger} = 0 = \hat{a}_{\alpha j} \hat{a}_{\alpha' j}$, we consider the two operators $(\hat{a}_{0j}^{\dagger} \hat{a}_{1j})$ and its conjugate $(\hat{a}_{1j}^{\dagger} \hat{a}_{0j})$. They are easily shown to satisfy Fermi anticommutation relations; this is true on the *same* site j : operators on *different* sites are still commuting. A full Fermi algebra can be recovered by means of the Jordan-Wigner transformation

$$\hat{c}_j = \exp \left(i\pi \sum_{\ell=1}^{j-1} \hat{n}_{\ell} \right) \hat{a}_{0j}^{\dagger} \hat{a}_{1j}, \tag{2}$$

where the Fermion number

$$\hat{n}_j \equiv \hat{c}_j^\dagger \hat{c}_j = \hat{n}_{1j} = 1 - \hat{n}_{0j} \quad (3)$$

takes values 1 and 0 that match the atom species populating site j . The Fermionic vacuum $|0\rangle_j$ corresponds to a 0-atom, while $|1\rangle_j$ is now interpreted as the one-Fermion state. Therefore, an overall generic state in \mathcal{H}_R takes the form of a superposition of 2^M base states,

$$|s\rangle = \sum_{\{\alpha_1, \dots, \alpha_M\}} \Gamma_{\alpha_1, \dots, \alpha_M} |\alpha_1 \dots \alpha_M\rangle. \quad (4)$$

The dynamics of the system in the Hilbert subspace \mathcal{H}_R follows from (1) and can be described by an effective Hamiltonian H_R which can be found by the method used in Refs. [4, 7]. The general H_R is obtained in Appendix B, while we reasonably assume here that in (1) the interaction constants do not depend on the atomic internal state, i.e., $U_0 = U_1 = U$ and $t_{0j} = t_{1j} \equiv t_j$, which eventually yields the following

$$H_R = - \sum_{j=1}^{M-1} \tau_j (\hat{c}_j^\dagger \hat{c}_{j+1} + \hat{c}_{j+1}^\dagger \hat{c}_j), \quad (5)$$

with $\tau_j = t_j^2/U$: indeed, as the expectation values of the hopping term in the Hamiltonian (1) vanish within \mathcal{H}_R , the possible dynamical processes occur at second order; in other words, to preserve site occupation two hoppings must occur. The Hamiltonian (5) describes the dynamics of a one-dimensional gas of free fermions; the dynamically active states are those with nonvanishing probability amplitude to have a fermion-hole pair in neighboring sites. As it commutes with the fermion-number operator $\hat{n}_F = \sum_j \hat{c}_j^\dagger \hat{c}_j$, the Hamiltonian (5) H_R is reducible: the irreducible subspaces of \mathcal{H}_R have an integer eigenvalue n_F of \hat{n}_F and dimension $\binom{M}{n_F}$.

2.2. The analogy

During an oscillation of the classical NC there are several spheres at rest and in contact with each other, and some moving spheres. When a moving sphere hits a sphere at rest, the latter keeps being at rest and exchanges its momentum with the nearby sphere (upper part of figure 1). In the quantum analogue of the NC we are discussing here, the role of the spheres' momenta is played by the wave-functions at each lattice site. Rather than the transfer of mechanical momentum, in the quantum system there is a transmission along the lattice of a disturbance of the wave-function. This is represented in the lower part of figure 1. Furthermore, in the place of the spheres oscillating at the boundaries of the chain, in our system we expect to observe the oscillation of the wave-function amplitude on the lattice ends due to the disturbance that runs forward and back. The system's wave function at each lattice site j can be a superposition of the two atomic internal states $|0\rangle_j$ and $|1\rangle_j$. Under the analogy we propose, one can for instance associate to the spheres at rest the states $|0\rangle_j$, and, accordingly, a moving sphere, let us say the first one, corresponds to a state $a|1\rangle_1 + b|0\rangle_1$, i.e., a superposition

of the two internal states. In terms of atoms this amounts to consider all sites initially populated by a species-0 atom, but for (a partial superposition with) a species-1 atom in the first site. This triggers oscillations whose dynamics is ruled by Hamiltonian (5), and essentially consist in the disturbance travelling along the lattice, i.e., the solitary species-1 atom propagates through the chain of species-0 atoms and migrates until the opposite end, where it is reflected back thus determining the NC effect. Remarkably, this analogue of the classical propagation is described in terms of fermions: the most ‘non-classical’ particles. Note that in both systems the effect of the propagation is perceived by ‘observing’ the lattice boundaries.

Suppose now that a Bose-Einstein condensate is adiabatically led into the Tonks-Girardeau regime with one atom per site and with all atoms in the same internal state, let's say the state $|0\rangle \equiv \prod_j |0\rangle_j$. The evolved state vector at time $t > 0$ is generally non-separable, and takes the general form of (4). Thanks to the fact that the Hamiltonian (5) is quadratic, one can exactly determine the time evolution for a generic initial condition. In what follows we are going to consider different dynamical scenarios that can show up, depending on the hopping amplitudes $\{\tau_j\}$.

To form an initial state in analogy with that of a classical NC, let us take that with all atoms in the internal state $|0\rangle_j$, and give a ‘kick’ only to the first atom, $|s(0)\rangle = \hat{c}_1^\dagger |0\rangle = |10\cdots 0\rangle$, corresponding to the first atom in the internal state $|1\rangle$ and all others in the internal state $|0\rangle$. Note that H_R commutes with the total number operator $\sum_j \hat{n}_j$ and therefore the state evolves in the one-excitation sector of \mathcal{H}_R .

To calculate the dynamics one has to diagonalize the Hamiltonian (5) in the form

$$H_R = \sum_{n=1}^M \omega_n \hat{\eta}_n^\dagger \hat{\eta}_n, \quad (6)$$

so the initial state evolves as $|s(t)\rangle = \sum_n g_{n1} e^{-i\omega_n t} \hat{\eta}_n^\dagger |0\rangle$ (see Appendix C). The probability amplitude to find a particle in the j -th site at time t is given by

$$A_j(t) \equiv \langle 0 | \hat{c}_j | s(t) \rangle = \sum_{n=1}^M g_{n1} g_{nj} e^{-i\omega_n t}, \quad (7)$$

and can be calculated numerically.

3. Two opposite schemes for a quantum Newton cradle

In this section we examine the possibility of realizing a QNC by means of the most natural choice of a simply uniform lattice. The simple theoretical treatment illustrates the mechanism underlying the cradle's oscillations as well as the reasons why this particular setup does not behave as expected. This is contrasted with a different *ad-hoc* arrangement of the hopping amplitudes, which, in spite of being difficult to attain in practice, shows that what is needed regards the frequency spectrum of the discrete system, namely that the frequencies be equally spaced.

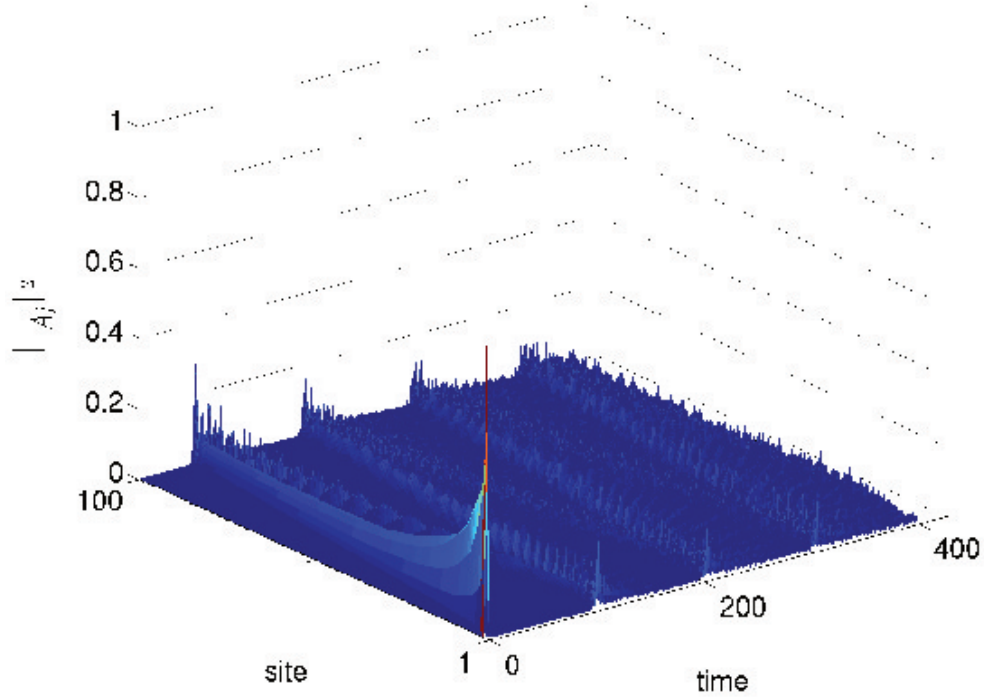


Figure 2. Disturbance of the wave-function that travels forward and backward along the chain.

3.1. Uniform QNC

This is the simplest case, both theoretically and experimentally, and occurs when all hopping amplitudes are equal, $\tau_j = \tau$, i.e., the chain is *uniform*. In this case one has [8] the orthogonal matrix $g_{nj} = \sqrt{\frac{2}{M+1}} \sin k_n j$ with $k_n = \frac{\pi n}{M+1}$ ($n = 1, \dots, M$) and the eigenvalues $\omega_n = -2 \cos k_n$; it follows that the evolving excitation is described by the sum

$$A_j(t) = \frac{2}{M+1} \sum_{n=1}^M \sin k_n j \sin k_n e^{2it \cos k_n}, \quad (8)$$

whose square modulus is reported in figure 2. It is clearly shown that the initial disturbance of the wave-function travels along the chain in the form of a wavepacket, which reaches the opposite end of the chain and is reflected backward. However, one can clearly see a significant attenuation of the transmitted signal, an effect essentially due to the destructive interference of the wave-function components. In other words, after a few bounces, namely in a time of the order of a multiple of M , the initial state $|1, 0 \dots 0\rangle$ evolves to a state where the species-1 boson is delocalized along the chain. This is the generic situation that occurs in a dispersive system: the wave-function spreads over the lattice during the time evolution until the initial wavepacket is lost. A similar phenomenon also occurs in the classical NC if the masses of the spheres are not identical, i.e., in the non-uniform case. Evidently, in the quantum analogue, the

uniformity of the system causes dispersion: therefore, it is important to identify under which conditions such attenuation can be minimized.

3.2. Perfect QNC

The dynamic decoherence described above can be not only reduced but even eliminated by letting the tunnelling amplitudes to vary along the chain with well-defined *nonuniform* values. In fact, in the field of quantum information theory it is known since a few years [9, 10, 11, 12] that a dispersionless end-to-end quantum-state transmission can be obtained, for a Hamiltonian like (5), when its nearest-neighbour couplings are suitably engineered, namely with proper values of the parameters $\{\tau_j\}$.

Looking at (7), it is indeed apparent that if all frequencies are ‘linear’, namely if $\omega_n = \Omega_0 + \Omega n$, then, setting the half-period time $t' = \pi/\Omega$, one finds that $A_j(2t') = e^{-2i\Omega_0 t'} A_j(0) = e^{-2i\Omega_0 t'} \delta_{j1}$, i.e., the initial state is exactly reproduced (up to an overall phase) and the dynamics has a period $2t'$. Furthermore, for a mirror-symmetric chain ($\tau_j = \tau_{M-j}$) one has alternatively mirror-symmetric/antisymmetric eigenvectors [13], $g_{n,M+1-j} = (-)^n g_{nj}$, and therefore

$$A_j(t') = e^{-i\Omega_0 t'} \delta_{jM}, \quad (9)$$

meaning that at the time t' the initial state is perfectly mirrored and the initial excitation $\hat{c}_1^\dagger|0\rangle$ is fully transferred to the opposite end of the chain $|s(t')\rangle = e^{-i\Omega_0 t'} \hat{c}_M^\dagger|0\rangle$. However, in order to obtain eigenvalues $\{\omega_n\}$ suitable for perfect transfer, the couplings $\{\tau_j\}$ must be individually engineered [9]. This can be rapidly proven by considering a spin- S subjected to a field along the x -direction, i.e., whose Hamiltonian is $H = \Omega \hat{S}^x = \frac{1}{2}\Omega(\hat{S}^+ + \hat{S}^-)$, with

$$S^+ = \sum_{m=-S}^S \sqrt{(S+1+m)(S-m)} |m+1\rangle\langle m|; \quad (10)$$

replacing $2S+1 = M$, $j = S+1-m$, and identifying $\hat{c}_j^\dagger|0\rangle = |S+1-j\rangle$, one exactly maps the uniform rotation $e^{-it\Omega\hat{S}^x}$ onto the perfect excitation transmission forth and back along the array with couplings $\tau_j = \Omega\sqrt{j(M-j)}$, which indeed yield equally spaced eigenvalues $\omega_n = \Omega(n - \frac{M-1}{2})$. So, in principle, there is a way to obtain a perfect quantum cradle, whose behaviour is illustrated in figure 3. Nevertheless, one has to recognize that its experimental realization by means of the accurate tuning of each tunnel coupling is an apparently hopeless task. It is worthwhile to mention that, in a different context, a cold-atom system undergoing the dynamics of a large rotating spin has been realized in [14].

4. Two realistic schemes for a quasi-perfect QNC

On the basis of the discussion in the preceding section, we are going here to show that it is possible to minimally modify the least demanding uniform lattice in order to strongly improve the cradle's performance. The main observation is that one can limit

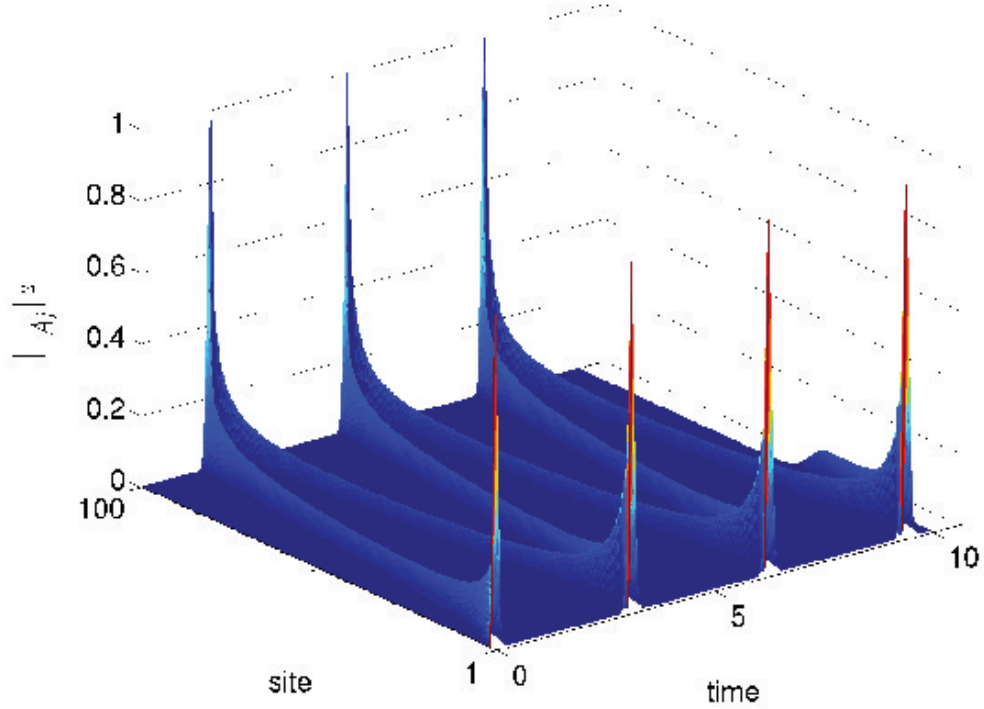


Figure 3. Disturbance of the wave-function that travels forward and backward along the suitably ‘adapted’ chain with $\tau_j \propto \sqrt{j(M-j)}$.

the requisite of a linear spectrum only to those modes which are actually activated by triggering a perturbation at an endpoint of the chain.

4.1. Quasi-uniform array

There exists a simpler way for the actual realization of a high-quality QNC in an essentially uniform chain, such that the need of engineering is littlest. A natural strategy, in order to move towards the shape of the hopping amplitudes of Sec. 3.2, is that of weakening the extremal τ_j ’s, for instance by acting with a transverse beam to increase the potential barriers between the endpoint wells of the optical lattice. Indeed, keeping the requirement of a mirror-symmetric chain [15], one can minimally modify a uniform chain taking equal couplings, $\tau_j = \tau$, but for the ones at the edges, $\tau_1 = \tau_{M-1} = x\tau$, with $x < 1$, and look for the best transfer conditions. In [8] it is shown that the eigenvalues can still be written as $\omega_n = -2\cos k_n$, but the pseudo-wavevectors

$$k_n = \frac{\pi n + 2\varphi_{k_n}}{M+1} \quad (n = 1, \dots, M), \quad (11)$$

varying in the interval $(0, \pi)$ are no more equally spaced, being affected by the *shifts*

$$\varphi_k = k - \cot^{-1} \left(\frac{x^2}{2-x^2} \cot k \right). \quad (12)$$

The discussion made above about the ideal case shows that a ‘linear’ dispersion relation guarantees coherent transmission of the initial excitation. However, the eigenvalues

$\omega_n = -2 \cos k_n$ of the quasi-uniform chain are almost linear just in a neighborhood of the inflection point, $k_n \sim \pi/2$. Looking more closely at the expression of the amplitude (7) at the last site, that, using the mirror-symmetry property $g_{n,M+1-j} = (-)^n g_{nj}$, reads

$$A_M(t) = \sum_{n=1}^M g_{n1}^2 e^{i(\pi - \omega_{k_n} t)}, \quad (13)$$

one can suppose that a good deal would be to have the prefactor g_{n1}^2 , which can be thought of as a normalized probability, strongly peaked just in the linear zone where $n \sim (M+1)/2$, in such a way that the dynamics involves coherent modes. We have seen that this is not the case for the fully uniform chain, because $g_{n1}^2 \sim \sin^2 k_n$ has its maximum in the desired zone but has too broad a shape. It is shown in [16] that the shape of g_{n1}^2 shrinks when x decreases. As expected, this effect improves (the absolute value of) the transmission amplitude (13) up to a maximum that depends on M : even for an infinitely long chain this optimal value is still finite and larger than 0.853, the optimal coupling being $x \simeq 1.03 M^{-1/6}$. When x gets smaller the distribution g_{n1}^2 gets narrower and narrower, however what prevents from getting perfect transfer is the obvious fact that by varying x one also affects the shape of the dispersion relation ω_{k_n} , perturbing its ‘quasi-linear’ behavior. It is natural to observe that, in order to have an almost independent control over these *two* effects (shrinking of the weighting density g_{n1}^2 and deformation of ω_{k_n}) *two* parameters are needed. As a matter of fact taking into play also the second bonds $\tau_2 = \tau_{M-2} = y\tau$ makes the difference and allows one to guarantee a response larger than 0.987 when the coupling are tuned as $x \simeq 2M^{-1/3}$ and $y \simeq 2^{3/4} M^{-1/6}$ [17]. Moreover, optimal response is obtained also in a wide neighborhood of the optimal couplings, so there is no need to fine-tune them.

4.2. Uniform array with a Gaussian trap

The last scheme we propose, considers a configuration that can be better realized in an experiment. Besides the uniform one-dimensional optical potential, we add a trapping potential that generates a site-dependent energy-offset ϱ_j , for $j = 1, \dots, M$, with a Gaussian profile (figure 4). Furthermore, we choose the initial state $|s(0)\rangle = \sum_j z_j \hat{c}_j^\dagger |0\rangle$, that represents a Gaussian wave-packet along the lattice. The site wave-function in fact is $z_j = A \exp(-(j - x_0)^2/\varsigma^2)$, where A is a normalization factor and x_0 and ς are the centre and the width of the packet, respectively.

Such a setup is a more realistic configuration with respect to the previous ones. In fact, in the schemes that we have illustrated so far, the bounce of the disturbance of the wave-function at the lattice ends, takes place because of the open-boundary conditions. On the contrary, in the present setup, the wave-packet oscillates inside the trapping potential and its speed inversion is caused by the forces generated by the trapping potential. In figure 5 it is evident that the packet never reaches the lattice ends. In fact, when the wave-packet moves from the trapping centre towards a lattice’s end, its speed is slowed down by the trapping potential, until the motion is inverted and the packet is accelerated in the opposite direction.

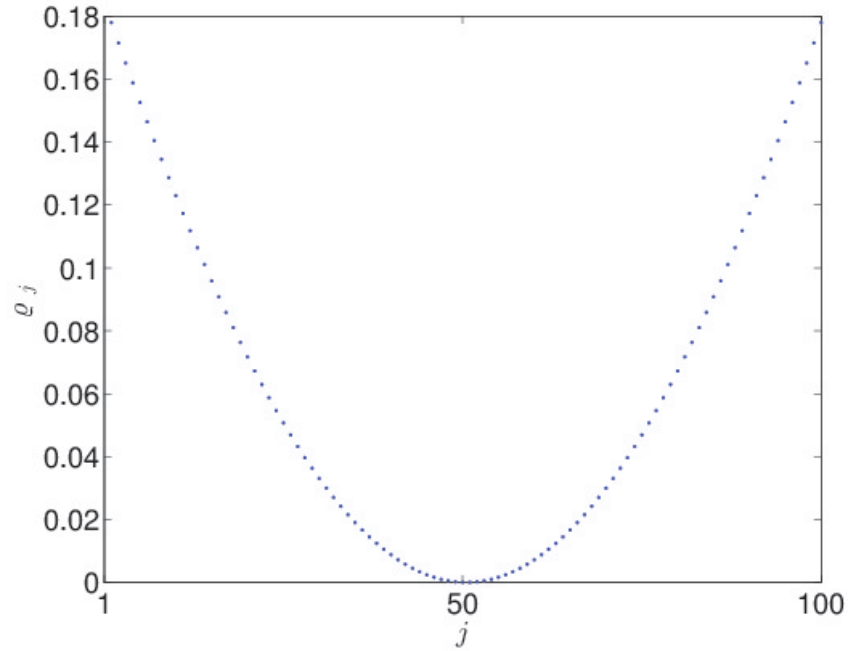


Figure 4. The trapping potential generates a site-dependent energy-offset ϱ_j , for $j = 1, \dots, M$. The figure shows ϱ_j as a function of the site index $j = 1, \dots, M$.

Figure 5 illustrates the result of a simulation made with an optical lattice of $M = 100$ sites and an initial state with $x_0 = 20$ and $\varsigma = 10$. The on-site energy offset is $\varrho_j = \exp(-(j - x_m)^2/\vartheta^2)$, with $x_m = 50$ and $\vartheta \approx 110$. The ‘dispersion relation’ ω_n shown in figure 6, displays intervals with approximately equal spacing, which is the condition leading to quasi-perfect transmission. To this goal, the initial state is taken as a narrow superposition of eigenmodes chosen in an almost linear region as shown in figure 6. Figure 5 proves indeed that the system displays a high transmission amplitude.

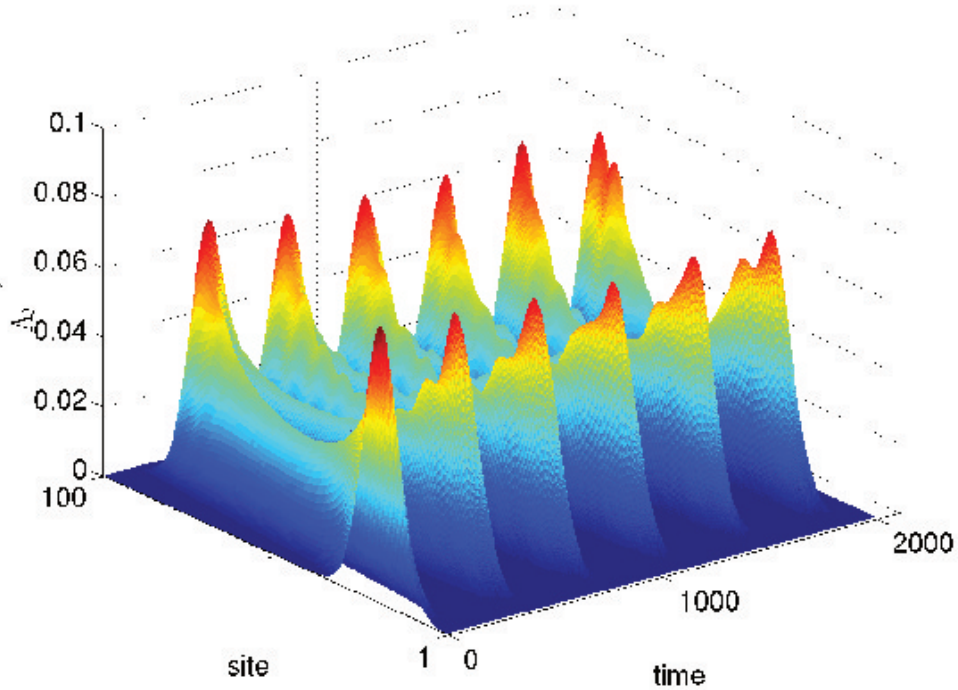


Figure 5. Disturbance of the wave-function that travels forward and backward in the uniform chain, $\{\tau_j = 1\}$, with a superimposed Gaussian confining potential. When the wave-packet moves toward a lattice's end, its speed is slowed down by the trapping potential, until the motion is inverted. Then the packet is accelerated in the opposite direction, as long as, it reaches the centre of the potential.

5. Conclusions

We have investigated an experimental framework that could realize a quantum analogue of Newton's cradle, starting from a Bose-Einstein condensate of two atomic species (i.e., atoms with two internal states) trapped in a one-dimensional tube with a longitudinal optical lattice; the system is kept in a strong Tonks-Girardeau regime with maximal filling factor, so that the lattice sites contain one atom and at each site the wave function is a superposition of the two internal atomic states. We have shown that the tunnelling between sites makes the system equivalent to a free-fermion gas on a finite lattice. In these conditions, one can trigger a disturbance of the wave function at one lattice end and this perturbation starts bouncing back and forth from the ends, just as the extremal spheres in the classical Newton's cradle: the analogy associates the propagation of a wave-function disturbance with the transmission of mechanical momentum.

However, in the quantum system the travelling wave undergoes decoherence, a phenomenon that makes a uniform lattice (i.e., with uniform tunnelling amplitudes) almost useless; still, it is known [9] that a suitable arrangement of the tunnelling amplitudes can even lead to a virtually perpetual cyclic bouncing. These possible schemes illustrate two opposite situations: the first is easy to realize but gives a scarce

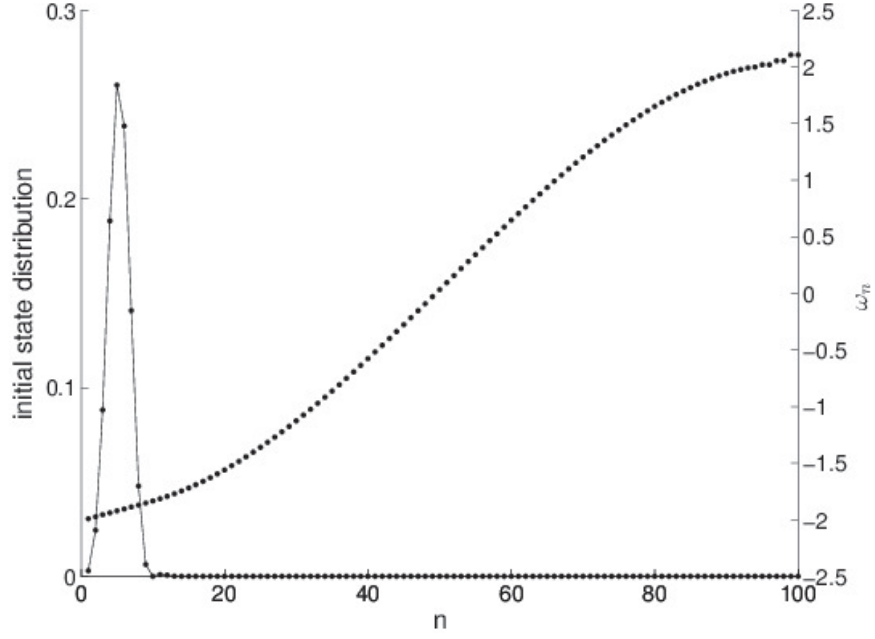


Figure 6. Eigenvalues ω_n in presence of the Gaussian trapping potential (right y -axis) and mode components of the initial state $|s(0)\rangle = \sum_j z_j \hat{c}_j^\dagger |0\rangle$ (left y -axis), showing that this state only involves a linear portion of the ‘dispersion relation’.

result, the latter would be perfect but requires an almost impossible engineering.

That’s why we looked for compromises that, minimizing the required experimental adaptation of the interactions, give almost perfect quantum Newton’s cradles. In this respect, we proposed two schemes: the first one involves a weakening of the extremal pairs of couplings and can lead to an amplitude response of 99%, i.e., the dynamics could be observed for tenths of oscillations; in the second we considered a longitudinal trapping potential with a Gaussian shape. Of course, the possibility to obtain quantum systems

that allow high-quality wave transmission is not only relevant from the speculative point of view, but also in the field of the realization of quantum devices like atomic interferometers, quantum memories, and quantum channels. Nevertheless, realizing the quantum Newton's cradle we proposed would be stirring by itself for the insight it would give into the entangled beauty of Quantum Mechanics.

Acknowledgments

R. F. thanks Vittorio Penna and Pierfrancesco Buonsante for their help in the present investigation.

Appendix A. Bose-Hubbard model

We start with a mixture of bosonic atoms with two different internal states, subjected to a strong transverse trapping potential with frequency $\omega_\perp \gg \mu/\hbar$, where μ is the chemical potential. The quantum dynamics of an ultracold dilute mixture of bosonic atoms with two internal states is described by the Hamiltonian operator

$$\begin{aligned} \hat{H} = & \sum_{\alpha=1}^2 \int d\mathbf{r} \hat{\psi}_\alpha^\dagger(\mathbf{r}) \left[-\frac{\hbar^2}{2m} \nabla^2 + V_{ext}^\alpha(\mathbf{r}) \right] \hat{\psi}_\alpha(\mathbf{r}) + \\ & \frac{\pi \hbar^2}{m} \sum_{\alpha, \beta=1}^2 a_{\alpha\beta} \int d\mathbf{r} \hat{\psi}_\alpha^\dagger(\mathbf{r}) \hat{\psi}_\beta^\dagger(\mathbf{r}) \hat{\psi}_\beta(\mathbf{r}) \hat{\psi}_\alpha(\mathbf{r}), \end{aligned} \quad (\text{A.1})$$

where α and β take the values 1, 2, corresponding to the internal states, the boson-field operator $\hat{\psi}_\alpha(\mathbf{r})$ ($\hat{\psi}_\alpha^\dagger(\mathbf{r})$) annihilates (creates) an atom at $\mathbf{r} = (r_x, r_y, r_z)$ in the internal state α . V_{ext}^α is the external trapping potential seen by the atoms in the state α . The nonlinear interaction term depends on the intraspecies and interspecies scattering lengths $a_{\alpha\beta}$, and on the atomic mass m . We consider the case of repulsive atomic interactions, thus $a_{\alpha\beta} > 0$ for $\alpha, \beta = 1, 2$. The external trapping potential of the optical lattice reads $V_{ext}^\alpha(\mathbf{r}) = V^\alpha \sin^2(k_L r_x) + m\omega_\perp^2(r_y^2 + r_z^2)/2$, where k_L is the laser mode which traps the atoms. Accordingly, the physics is effectively one-dimensional. Following [18, 19], (A.1) is transformed into an effective quantum (Bose-Hubbard) Hamiltonian that describes, within the second quantization formalism, the boson mixture dynamics in an optical lattice. The boson-field operator can be rewritten in terms of the Wannier functions $u_j^\alpha(\mathbf{r})$ as (see [18])

$$\hat{\psi}_\alpha(\mathbf{r}, t) = \sum_{j=1}^M u_j^\alpha(\mathbf{r}) \hat{a}_{\alpha j}(t), \quad (\text{A.2})$$

where the boson operator $\hat{a}_{\alpha j}$ ($\hat{a}_{\alpha j}^\dagger$) destroys (creates) an atom in the internal state α at the lattice site j . By substituting (A.2) into Hamiltonian (A.1), and keeping the lowest order in the overlap between the single-well wave functions, one obtains the effective one-dimensional Bose-Hubbard Hamiltonian (1). Where, U and U_1, U_2 are the inter- and intra-species onsite interaction energy, respectively, and t_α is the hopping amplitude of

the species α . These constants can be estimated, e.g., in the tight-binding approximation one obtains $U_\alpha = 2\pi\hbar^2 a_{\alpha\alpha}/m \int dx |u_j^\alpha|^4$ and $t_\alpha = -2 \int dx \bar{u}_j^\alpha [\frac{\hbar^2}{2m} \nabla^2 + V_{ext}^\alpha] u_{j+1}^\alpha$ [18].

Appendix B. Fermionization

Considering the limit of strong on-site repulsion (large U 's) we can separate from the Hamiltonian (1) a perturbative term V , writing $H = H_0 + V$. Thus, up to an irrelevant constant factor it results

$$H_0 = \sum_j [U_0 \hat{n}_{0j}(\hat{n}_{0j}-1) + U_1 \hat{n}_{1j}(\hat{n}_{1j}-1) + \frac{U}{2}(2\hat{n}_{0j}\hat{n}_{1j} + 1 - \hat{n}_{0j} - \hat{n}_{1j})] \quad (\text{B.1})$$

$$V = -\sum_{j=1}^{M-1} [t_{0j} \hat{a}_{0j}^\dagger \hat{a}_{0,j+1} + t_{1j} \hat{a}_{1j}^\dagger \hat{a}_{1,j+1} + \text{h.c.}] . \quad (\text{B.2})$$

The recipe for the effective Hamiltonian restricted to the Hilbert space \mathcal{H}_R of the states for which the expectation value of H_0 vanishes (i.e., $\hat{n}_{0j} + \hat{n}_{1j} = 1$) is [4, 20, 7]

$$\langle \alpha | H_R | \beta \rangle = - \sum_\psi \frac{\langle \alpha | V | \psi \rangle \langle \psi | V | \beta \rangle}{\langle \psi | H_0 | \psi \rangle} , \quad (\text{B.3})$$

where the virtual states ψ are necessarily outside \mathcal{H}_R . In order that $V|\psi\rangle \in \mathcal{H}_R$ both matrix elements in V must involve the same site pair $(j, j+1)$; for each pair, out of 16 possible terms, 6 do not vanish and it turns out that the effective interaction can be eventually written as

$$H_R = \sum_{j=1}^{M-1} [-\tau_j (\hat{b}_j^\dagger \hat{b}_{j+1} + \hat{b}_{j+1}^\dagger \hat{b}_j) + \gamma_j \hat{b}_j^\dagger \hat{b}_j \hat{b}_{j+1}^\dagger \hat{b}_{j+1} + \sigma_j (\hat{b}_j^\dagger \hat{b}_j + \hat{b}_{j+1}^\dagger \hat{b}_{j+1})] , \quad (\text{B.4})$$

where a further additive constant is neglected and

$$\tau_j = 2 \frac{t_{0j} t_{1j}}{U} , \quad \gamma_j = 2 \left[\frac{t_{0j}^2 + t_{1j}^2}{U} - \frac{t_{0j}^2}{U_0} - \frac{t_{1j}^2}{U_1} \right] \quad (\text{B.5})$$

$$\sigma_j = 2 \frac{t_{0j}^2}{U_0} - \frac{t_{0j}^2 + t_{1j}^2}{U} ; \quad (\text{B.6})$$

$\hat{b}_j = \hat{a}_{0j}^\dagger \hat{a}_{1j}$ and \hat{b}_j^\dagger are operators in \mathcal{H}_R such that $\{\hat{b}_j, \hat{b}_j^\dagger\} = 1$, while between different sites all commutators vanish. In the one-dimensional case they can be converted into Fermion operators by the transformation (2); if the interactions do not depend on the atomic internal state H_R turns into (5).

Appendix C. Time evolution

The exact eigenstates of Hamiltonian (5) are derived by means of a linear transformation, $\hat{\eta}_n = g_{nj} \hat{c}_j$ and $\hat{\eta}_n^\dagger = g_{nj}^* \hat{c}_j^\dagger$. Requiring it to be canonical, i.e., imposing $\{\hat{\eta}_n, \hat{\eta}_{n'}^\dagger\} = \delta_{nn'}$,

one finds that the $M \times M$ matrix g_{nj} must be unitary, $g^\dagger g = gg^\dagger = \mathbb{1}$. Actually, g is also real (hence, orthogonal), as it diagonalizes the real symmetric matrix $A_{jj'} = (\tau_j \delta_{j+1,j'} + \tau_{j'} \delta_{j-1,j'})$, i.e., $\sum_{jj'} g_{nj} A_{jj'} g_{n'j'} = \omega_n \delta_{nn'}$; the diagonalized Hamiltonian has the form (6). When most of the couplings τ_j are equal, a convenient general method for solving the eigenvalue problem can be found in [8].

References

- [1] Kinoshita T, Wenger T and Weiss D S 2006 *Nature* **440** 900
- [2] Paredes B, Widera A, Murg V, Mandel O, Fölling S, Cirac I, Shlyapnikov G V, Hänsch T W and Bloch I 2004 *Nature* **429** 277
- [3] Mandel O, Greiner M, Widera A, Rom T, Hänsch T W and Bloch I 2003 *Nature* **425** 937
- [4] Kuklov A B and Svistunov B V 2003 *Phys. Rev. Lett.* **90** 100401
- [5] Altman E, Hofstetter W, Demler E and Lukin M D 2003 *New J. Physics* **5** 113,
- [6] Söyler Ş G , Capogrosso-Sansone B, Prokof'ev N V and Svistunov B V 2009 *New J. Physics* **11** 073036
- [7] Pachos J K and Rico E 2004 *Phys. Rev. A* **70** 053620
- [8] Banchi L and Vaia R 2013 *J. Math. Phys.* **54** 043501
- [9] Christandl M, Datta N, Ekert A, and Landahl A J 2004 *Phys. Rev. Lett.* **92** 187902
- [10] Christandl M, Datta N, Dorlas T C, Ekert A, Kay A and Landahl A J 2005 *Phys. Rev. A* **71** 032312
- [11] Karbach P and Stolze J 2005 *Phys. Rev. A* **72** 030301
- [12] Wang Y, Shuang F, and Rabitz H 2011 *Phys. Rev. A* **84** 012307
- [13] Cantoni A and Butler P 1976 *Linear Algebra Appl.* **13** 275
- [14] Petrovic J, Herrera I, Lombardi P, Schäfer F, Cataliotti F S 2013 *New J. Phys.* **15** 043002
- [15] Kay A 2010 *Int. J. Quan. Info.* **8** 641
- [16] Banchi L, Apollaro T J G, Cuccoli A, Vaia R, and Verrucchi P 2011 *New J. Phys.* **13** 123006
- [17] Banchi L, Apollaro T J G, Cuccoli A, Vaia R, and Verrucchi P 2012 *Phys. Rev. A* **85** 052319
- [18] Jaksch D, Bruder C, Cirac J I, Gardiner C W, and Zoller P 1998 *Phys. Rev. Lett.* **81** 3108
- [19] Jaksch D and Zoller P 2005 *Ann. Phys.* **315** 52-79
- [20] Duan L-M, Demler E, and Lukin M D 2003 *Phys. Rev. Lett.* **91** 090402